JOURNAL OF SOLID STATE CHEMISTRY **128,** 267–272 (1997)
ARTICLE NO. SC967217

Ambient and High-Pressure Structures of $LiMnVO_4$ and Its Mn^{3+}/Mn^{2+} Redox Energy

A. K. Padhi,[1] W. B. Archibald, K. S. Nanjundaswamy, and J. B. Goodenough

Center for Materials Science and Engineering, ETC 9.102, The University of Texas at Austin, Austin, Texas 78712-1063

Received August 20, 1996; in revised form October 29, 1996; accepted November 6, 1996

$LiMnVO_4$ has been prepared and shown, by Rietveld analysis, to be orthorhombic isostructural with $Li_{1.2}In_{0.6}VO_4$; it has a melting point of 784°C, and it transforms under a pressure of 55 kbar at 850°C to a 7.7% more dense cubic spinel phase $V[LiMn]O_4$. The orthorhombic phase contains linear, ferromagnetic chains of Mn^{2+} ions in edge-shared oxygen octahedra. The spinel has mostly octahedral Mn^{2+} ions with evidence, below 50 K, of ferrimagnetic clusters associated with some terahedral-site Mn^{2+}. Electrochemical delithiation of the spinel reveals a Mn^{3+}/Mn^{2+} couple located at ~ 3.8 eV below the Fermi energy of elemental lithium, which indicates that the $(VO_4)^{3-}$ tetrahedron behaves as a polyanion. This energy compares with 4.2 and 4.8 eV for the Co^{3+}/Co^{2+} and Ni^{3+}/Ni^{2+} couples in $V[LiCo]O_4$ and $V[LiNi]O_4$, respectively. © 1997 Academic Press

INTRODUCTION

Identification of compounds that transform under pressure into dense phases such as spinel is of importance for theories of the earth's mantle. Such transformations can account in part for sudden increases in the mantle's density that have become evident in seismic data.

A large number of compounds of the type $LiM^{2+}M'^{5+}O_4$, M = Be, Mg, Co, Ni, Zn, and Cd and M = V, Sb, and Nb have been investigated (1). $V[LiCo]O_4$ and $V[LiNi]O_4$ crystallize in the spinel structure at atmospheric pressure, where $V[LiCd]O_4$ is reported to have a pseudo-olivine structure (throughout, cations in square brackets occupy octahedral sites, those unbracketed occupy tetrahedral sites of the oxygen array). $V[LiMg]O_4$ has the olivine structure at atmospheric pressure and, like the olivines $Ge[Mg_2]O_4$ (2) and $Si[Mg_2]O_4$ (3), it transforms to the cubic spinel structure under pressure. The actual olivine structure contains a slightly distorted hexagonal-closed-packed oxygen array while the spinel has somewhat more dense and a slightly distorted cubic-closed-packed oxygen array. Phenacite, on the other hand, has a more open oxygen array with cations occupying only tetrahedral sites as in $LiBeVO_4$ which does not transform to spinel even under very high pressure; however, $LiZnVO_4$, with phenacite structure becomes a cubic spinel $V[LiZn]O_4$ under pressure. The phenacite–spinel transformation of $LiZnVO_4$ is the only one of its kind reported. Unlike V^{5+}, which was always found in a tetrahedral coordination, the Sb^{5+} and Nb^{5+} cations were found only in octahedral sites of the spinel structure. The mixed spinels $Co_{1-x}Li_x[Co_xLi_{1-x}Sb]O_4$ and $Zn_{1-x}Li_x[Zn_xLi_{1-x}Sb]O_4$ had ordered Sb^{5+} on the octahedral sites as evidenced by the superstructure lines in the powder X-ray diffraction patterns, and $Zn[LiNb]O_4$ has a tetragonal ($c/a = 1.38$) spinel structure. In this paper the synthesis and structure determination of an orthorhombic $LiV[Mn]O_4$ phase, which has two of the three cations in tetrahedral sites, and its transformation under pressure into the cubic spinel $V[LiMn]O_4$ structure are discussed. As part of an ongoing mapping of the redox energies relative to a lithium anode of octahedral-site cations in different environments, we also determine the Mn^{3+}/Mn^{2+} redox couple in the spinel phases and compare it with the Co^{3+}/Co^{2+} and Ni^{3+}/Ni^{2+} couples in the analogous spinels $V[LiCo]O_4$ and $V[LiNi]O_4$ attained by lithium extraction. Insertion of up to 7 lithium into the $V[LiCo]O_4$ and $V[LiNi]O_4$ spinels has been reported (4); the amorphous product would consist of Li_2O with metallic vanadium and cobalt or nickel. We find a similar result for $V[LiMn]O_4$.

EXPERIMENTAL PROCEDURE

The ambient-pressure orthorhombic phase of $LiV[Mn]O_4$ was prepared from stoichiometric amounts of $MnCO_3 \cdot 0.4H_2O$, Li_2CO_3, and V_2O_5 by direct solid-state reaction in prepurified argon atmosphere. After an initial decomposition of the mixed products at 250°C, the mixture was ground, pelletized, and fired at 700°C for 24 h in argon. The sample was slow cooled and crushed into powder for X-ray analysis.

[1] To whom correspondence should be addressed.

0022-4596/97 $25.00

A single-phase orthorhombic powder of $LiV[Mn]O_4$ was pelletized and sintered at 650°C, then it was encapsulated in gold foil for use in a "belt"-type high-pressure apparatus. The temperature inside the pressure chamber was determined from a calibrated curve of heater input power versus temperature. High-pressure experiments were carried out for pressures $10 \leq P \leq 55$ kbars near 850°C; the high-pressure phase was quenched in by shutting off the graphite-heater input power before releasing the pressure.

The electrochemical lithium extraction and insertion was done in a coin cell with a lithium-foil anode. The cathode material was ground to fine particles and blended with acetylene black and polytetrafluoroethylene (PTFE) in the ratio 70 : 25 : 5. Next, the sample was heated as a mixture for a few hours in an oven kept at 140°C before being pelletized with a hand press having properly spaced rollers. The electrolyte used was 1 *M* $LiClO_4$ in a one-to-one ratio (by volume) mixture of propylene carbonate (PC) and dimethoxyethane (DME). The cell was charged and discharged between minimum and maximum cell-voltage limits of 3.0 and 4.3 V at a current density 0.02 mA/cm^2 (0.5 mA/g).

Magnetic susceptibility versus temperature curves were obtained with a Quantum Design SQUID magnetometer. X-ray analysis was performed on a Philips Model APD 3520 powder diffractometer using Cu$K\alpha$ radiation with Si as the internal standard, and Rietveld refinements of the structures were done with a PC version of the DBWS program. Differential thermal analysis (DTA) was accomplished with a Perkin–Elmer Series 7 thermal analysis system.

RESULTS AND DISCUSSION

A Rietveld refinement of the orthorhombic phase of $LiMnVO_4$ was done on the data of 6001 reflections in the range covering $10^\circ < 2\theta < 130^\circ$ obtained at a basic 6-s count rate with a monochromatized beam of Cu$K\alpha$ radiation. The starting parameters were those of $LiV[Li_{0.2}In_{0.6}]O_4$[5] having the space group *Cmcm*. The refinement converged to the parameters shown in Table 1; the bond lengths and angles are given in Table 2. The lattice parameters are $a = 5.7611(1)$ Å, $b = 8.7462(1)$ Å, and $c = 6.3502(1)$ Å. In this structure, illustrated in Fig. 1, chains of edge-shared MnO_6 octahedra running parallel to the *c* axis are bridged by antiparallel pairs of edge-shared LiO_4 and VO_4 tetrahedra, and the V^{5+} ions are displaced less from the shared O(1)–O(1) edge than are the larger Li^+ ions.

TABLE 1
Positional and Isotropic Displacement Parameters for Orthorhombic Phase of $LiMnVO_4$

Atoms	Occupancy	Site	*x*	*y*	*z*	*B*(Å^2)
Mn	1.0	4*a*	0.0000	0.0000	0.0000	0.80 (7)
V	1.0	4*c*	0.0000	0.3574(3)		
					0.2500	0.57 (6)
Li	1.0	4*c*	0.5000	0.1669(1)		
					0.2500	2.30 (11)
O1	1.0	8*g*	0.2306(8)			
				0.4785(6)		
					0.2500	1.65 (9)
O2	1.0	8*f*	0.0000	0.2568(5)		
					0.0347(8)	
						1.05 (10)
R_p	11.98					
R_{wp}	15.19					
S	3.78					
D–WD	0.49					

TABLE 2
Bond Lengths (Å) and Angles (°) from Rietveld Refinement of Orthorhombic Phase $LiMnVO_4$

Mn octahedron			
Mn–O(1)	2.234(4) × 4		
Mn–O(2)	2.256(5) × 2		
O(1)*a*–Mn–O(1)*b*	179.9	O(1)*a*–Mn–O(1)*c*	88.0(1)
O(1)*a*–Mn–O(1)*d*	92.0(1)	O(1)*a*–Mn–O(2)*a*	90.8(1)
O(1)*a*–Mn–O(2)*b*	89.2(1)	O(1)*b*–Mn–O(1)*c*	92.0(1)
O(1)*b*–Mn–O(2)*a*	89.2(1)	O(1)*b*–Mn–O(2)*b*	90.8(1)
O(1)*c*–Mn–O(1)*d*	179.9(1)	O(1)*c*–Mn–O(2)*a*	90.8(1)
O(1)*c*–Mn–O(2)*b*	89.2(1)	O(1)*d*–Mn–O(2)*a*	89.2(1)
O(1)*d*–Mn–O(1)*b*	90.8(1)	O(2)*a*–Mn–O(2)*c*	180(1)
V tetrahedron			
V–O(1)	1.699(7) × 2		
V–O(2)	1.632(7) × 2		
O(1)*e*–V–O(1)*f*	102.9(1)	O(1)*e*–V–O(2)*c*	109.6(1)
O(1)*e*–V–O(2)*c*	109.6(1)	O(1)*f*–V–O(2)*c*	109.6(1)
O(1)*f*–V–O(2)*d*	109.6(1)	O(2)*c*–V–O(2)*d*	114.8(1)
Li tetrahedron			
Li–O(1)	2.116(1) × 2		
Li–O(2)	1.936(3) × 2		
O(1)*g*–Li–O(1)*c*	77.8(3)	O(1)*g*–Li–O(2)*e*	105.6(1)
O(1)*g*–Li–O(2)*f*	105.6(1)	O(1)*c*–Li–O(2)*e*	105.6(1)
O(1)*c*–Li–O(2)*f*	105.6(1)	O(2)*e*–Li–O(2)*f*	139.7(3)

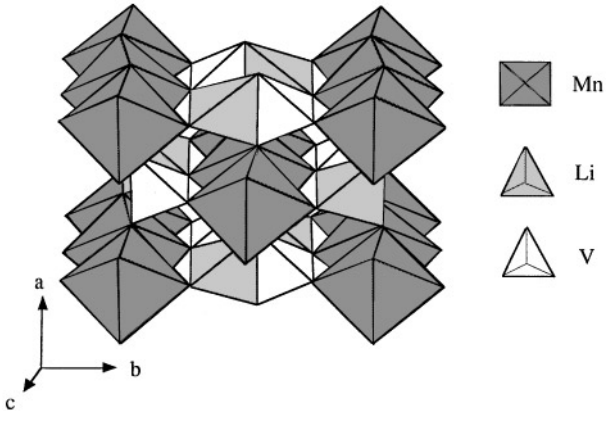

FIG. 1. Crystal structure of orthorhombic phase, $Li[Mn]VO_4$.

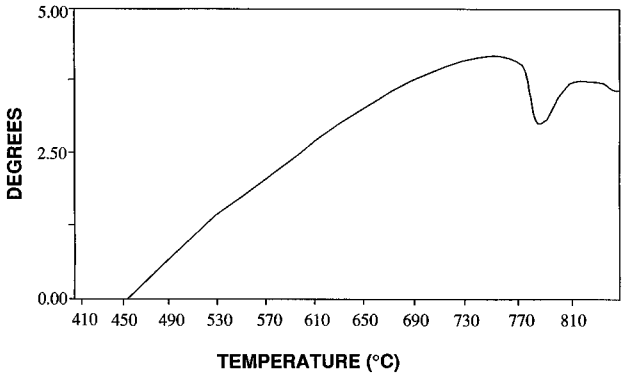

FIG. 2. DTA plot of $Li[Mn]VO_4$.

The DTA of Fig. 2 gave a melting point for the orthorhombic $LiV[Mn]O_4$ phase of 784°C; there was no other phase change to 800°C. The melting point increases with pressure, and the high-pressure spinel phase of $V[LiMn]O_4$ was obtained at a $P = 55$ kbars at a temperature of 850°C. Rietveld refinement of the high-pressure spinel phase, space group $Fd\bar{3}m$, showed a transition-metal (assumed to be V since the V^{5+} occupy tetrahedral sites and the Mn^{2+} octahedral sites in the orthorhombic parent phase) in the tetrahedral 8*a* sites with Mn and Li randomly distributed on the octahedral 16*d* sites. The powder X-ray diffraction patterns for both the phases are shown in Fig. 3; the (111) Bragg peak is much weaker than the (220) peak, contrary to what is found in $Li[Mn_2]O_4$, because Li is replaced by V in the tetrahedral sites. The lattice parameter $a = 8.4071(2)$ Å with $u = 0.2351(1)$. The converged parameters for the high-pressure spinel phase is given in Table 3. Bond lengths and bond angles are given in Table 4.

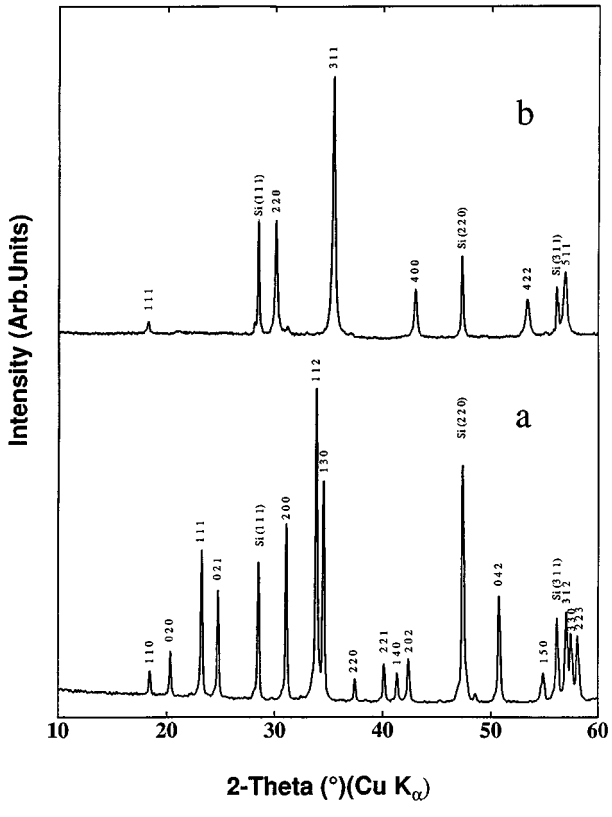

FIG. 3. XRD patterns of (a) orthorhombic $Li[Mn]VO_4$ (b) spinel $V[LiMn]O_4$.

TABLE 3
Positional and Isotropic Displacement Parameters for Spinel Phase of $LiMnVO_4$

Atoms	Occupancy	Site	*x*	*y*	*z*	*B* (Å^2)
Mn	0.5	16*d*	0.5000	0.5000	0.5000	0.31 (5)
V	1.0	8*a*	0.2500	0.2500	0.2500	0.72 (6)
Li	0.5	16*d*	0.5000	0.5000	0.5000	0.72 (6)
O	1.0	8*g*	0.2351(4)	0.2351(4)	0.2351(4)	1.48(11)
R_p	13.00					
R_{wp}	17.05					
S	2.60					
D–WD	1.14					

The paramagnetic susceptibility shows Curie–Weiss behavior above 100 K with a negative Weiss constant for the spinel and a positive Weiss constant for the othorhombic phase; both phases have a μ_{eff} close to the theoretical spin-only value for Mn^{2+} ions (Fig. 4). Antiferromagnetic Mn–Mn interactions between the Mn^{2+} ions, and hence a negative Weiss constant, are expected from superexchange theory for the half-filled d orbitals of a high spin Mn^{2+} ion. However, the 90° Mn–O–Mn interactions in both structures

TABLE 4
Bond Lengths (Å) and Angles (°) from Rietveld Refinement of Spinel Phase of $LiMnVO_4$

	($\frac{1}{2}$ Mn, $\frac{1}{2}$ Li) octahedron)		
($\frac{1}{2}$Mn, $\frac{1}{2}$Li)–O	2.234(4) × 6		
O(i)–($\frac{1}{2}$Mn, $\frac{1}{2}$Li)–O(ii)	180.0	O(i)–($\frac{1}{2}$Mn, $\frac{1}{2}$Li)–O(iii)	83.76 (12)
O(i)–($\frac{1}{2}$Mn, $\frac{1}{2}$Li)–O(iv)	96.24 (12)	O(i)–($\frac{1}{2}$Mn, $\frac{1}{2}$Li)–O(v)	83.76 (12)
O(i)–($\frac{1}{2}$Mn, $\frac{1}{2}$Li)–O(vi)	96.24 (12)	O(ii)–($\frac{1}{2}$Mn, $\frac{1}{2}$Li)–O(iii)	96.24 (12)
O(ii)–($\frac{1}{2}$Mn, $\frac{1}{2}$Li)–O(iv)	83.76 (12)	O(ii)–($\frac{1}{2}$Mn, $\frac{1}{2}$Li)–O(v)	96.24 (12)
O(ii)–($\frac{1}{2}$Mn, $\frac{1}{2}$Li)–O(vi)	83.76 (12)	O(iii)–($\frac{1}{2}$Mn, $\frac{1}{2}$Li)–O(iv)	180.0
O(iii)–($\frac{1}{2}$Mn, $\frac{1}{2}$Li)–O(v)	96.24 (12)	O(iii)–($\frac{1}{2}$Mn, $\frac{1}{2}$Li)–O(vi)	83.76 (12)
O(iv)–($\frac{1}{2}$Mn, $\frac{1}{2}$Li)–O(v)	83.76 (12)	O(iv)–($\frac{1}{2}$Mn, $\frac{1}{2}$Li)–O(vi)	96.24 (12)
O(iv)–($\frac{1}{2}$Mn, $\frac{1}{2}$Li)–O(v)	180.0		
	V tetrahedron		
V–O	1.603(6) × 2		
V–O	1.6032(19) × 2		
O(a)–V–O(b)	109.5	O(a)–V–O(c)	109.47 (10)
O(a)–V–O(d)	109.47 (10)	O(b)–V–O(c)	109.47 (10)
O(b)–V–O(d)	109.47 (10)	O(c)–V–O(d)	109.5 (3)

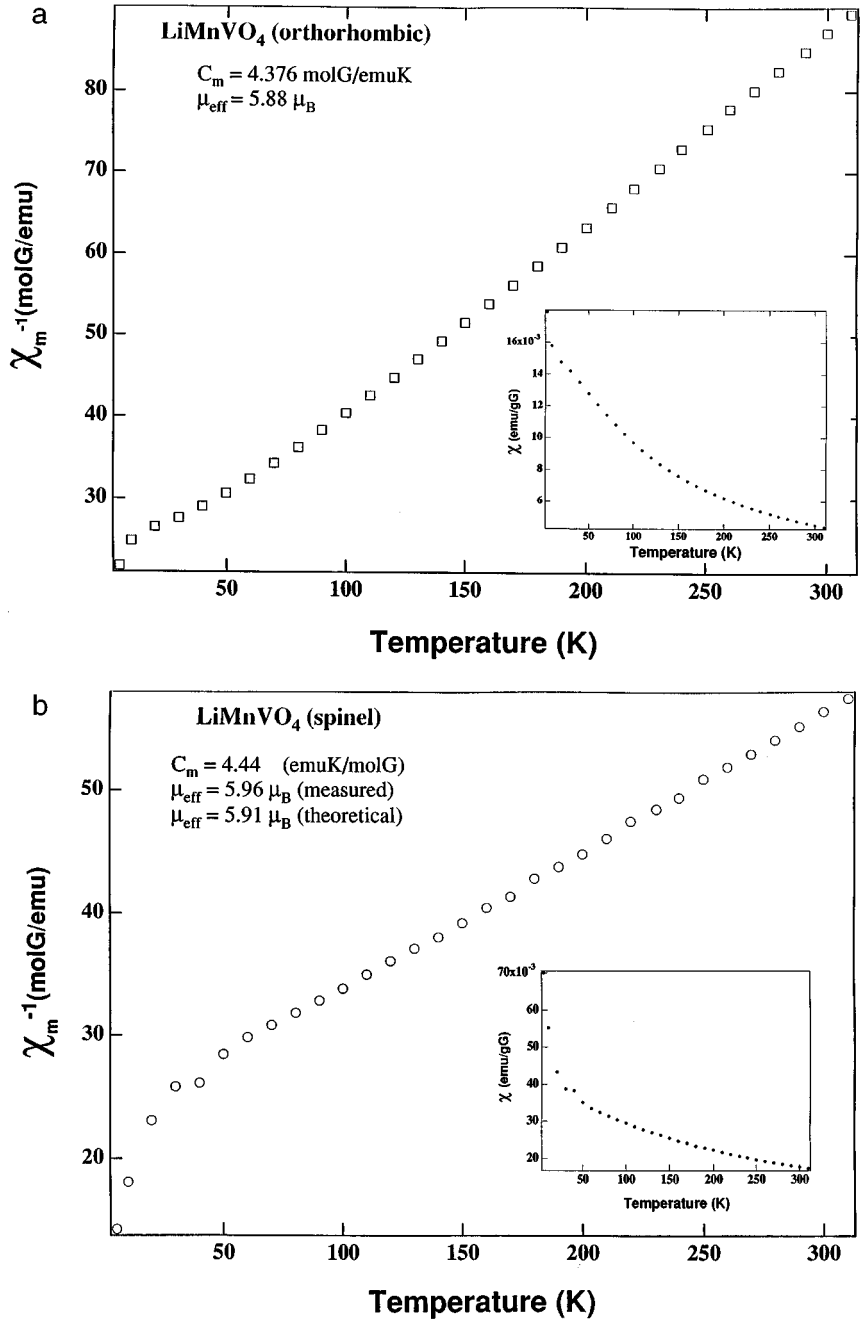

FIG. 4. Inverse of magnetic susceptibility versus temperature plots for (a) spinel $V[LiMn]O_4$ (b) orthorhombic $Li[Mn]VO_4$.

would be ferromagnetic by direct exchange between orthogonal orbitals. The Mn–Mn interactions are weaker in the othorhombic phase, which allows a longer Mn–Mn separation. Orthorhombic $LiV[Mn]O_4$ shows evidence of considerable short-range order in the edge-shared MnO_6 linear chains below 100 K, long-range antiferromagnetic order setting in only at lowest temperatures. The spinel with nominal formula $V[LiMn]O_4$ has an increase in susceptibility at lowest temperatures that is typical of a ferrimagnet, which indicates the presence of some Mn on the tetrahedral sites, $V_{1-x}Mn_x[LiV_xMn_{1-x}]O_4$.

Topotactic and reversible lithium insertion/extraction reactions have been demonstrated for a variety of spinels, including Fe_3O_4 (6), Mn_3O_4 (7), Co_3O_4 (8), $Li[Mn_2]O_4$ (9), $Li[Ti_2]O_4$ (10), and $Li[V_2]O_4$ (11). Of particular interest for the design of a secondary-battery electrode is the

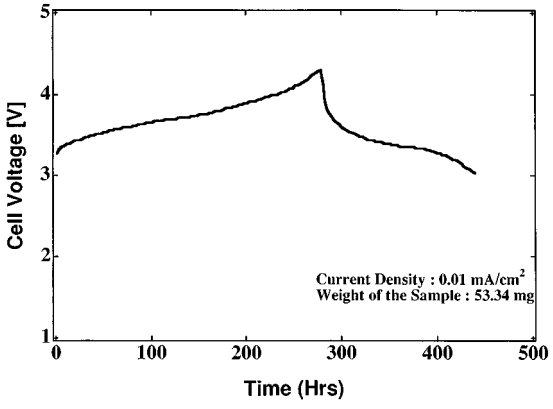

FIG. 5. Charge and discharge curves for spinel $V[LiMn]O_4$/$LiClO_4$ + PC + DME/Li coin-type cell at 0.5 mA/g (0.02 mA/cm^2).

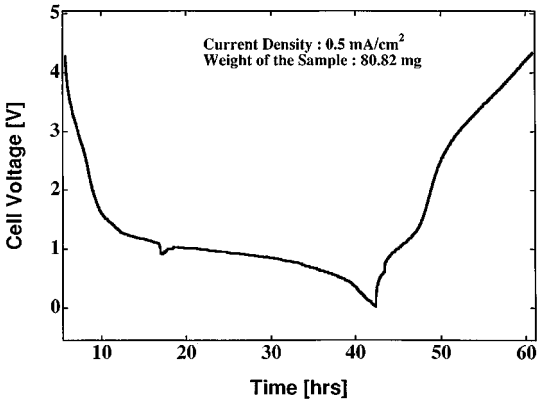

FIG. 6. Discharge and charge curve for orthorhombic $Li[Mn]VO_4$ at 0.5 mA/cm^2 (10 mA/g).

placement of the redox energies in the spinel structure and how these energies are shifted with the location of the Li^+ ions and with the presence of different counter cations. A reversible insertion of Li into the family $Li[MnM]O_4$ (M = Cr, Co, or Ni) has been used to investigate the influence of an octahedral-site counter cation (12). Reversible extraction of lithium from $V[LiCo]O_4$ and $V[LiNi]O_4$ has shown plateaus at 4.2 and 4.8 V versus a lithium anode in the $V(x)$ curve for the Co^{3+}/Co^{2+} and Ni^{3+}/Ni^{2+} redox couples, respectively (13). We have extended these measurements to the high-pressure spinel phase $V[LiMn]O_4$ to include the relative energy of the Mn^{3+}/Mn^{2+} couple for comparison.

About 0.6 Li per formula unit could be reversibly extracted from the nominal spinel $V[LiMn]O_4$. Figure 5 shows the charge and discharge curves taken at 0.02 mA/cm^2 (0.5 mA/g); the difference in the midpoints of the curves at $\sim$4.1 and 3.6 reflects the relatively large overvoltage associated with extraction of Li. The large overvoltage is due to the fact that the lithium atoms must be extracted from a disordered array of Li and Mn atoms on the 16*d* octahedral sites. We conclude that the M^{3+}/M^{2+} redox couples for M = Mn, Co, and Ni in the nominal spinels $V[LiM]O_4$ stand in the relation 3.8, 4.2, and 4.8 eV below the Fermi energy of elemental lithium. Such a sequence is consistent with the octahedral-site redox couples found for these ions in other structures (14). Moreover, a shift from 3.0 eV for the Mn^{4+}/Mn^{3+} couple in the spinel $Li[Mn_2]O_4$ to 3.8 eV for the Mn^{3+}/Mn^{2+} couple in nominal $V[LiMn]O_4$ demonstrates that the VO_4-tetrahedral unit may be considered to be a $(VO_4)^{3-}$ polyanion. The strong V–O covalent bonding remarkably stabilizes the octahedral-site redox energies, as has been noted for the other polyanions such as $(SO_4)^{2-}$, $(PO_4)^{3-}$ (15).

Lithium extraction from the orthorhombic $LiV[Mn]O_4$ proved difficult, as should be expected from the structure. On discharge, it was possible to introduce three lithium atoms per formula unit but not reversibly as shown in Fig. 6.

CONCLUSION

$LiMnVO_4$ is shown to exist in two forms: an ambient-pressure $LiV[Mn]O_4$, isostructural with $Li_{1.2}In_{0.6}VO_4$, and a high-pressure (P = 55 kbar) cubic-spinel phase $V[LiMn]O_4$ about 7.7% more dense in which $(VO_4)^{3-}$ ions act as polyanions. There may be some tetrahedral-site Mn^{2+} in nominal $V[LiMn]O_4$ as evidenced by the ferrimagnetic behavior below 50 K. The chains of edge-shared MnO_6 octahedra in $LiV[Mn]O_4$ are antiferromagnetic. The redox energy of the Mn^{3+}/Mn^{2+} couple lies 3.8 eV below the Fermi energy of elemental lithium. This represents a remarkable stabilization from its position discretely above the Mn^{4+}/Mn^{3+} redox energy at 3.0 eV relative to lithium in $Li[Mn_2]O_4$.

ACKNOWLEDGMENTS

We thank Professors Hugo Steinfink and S. Balakrishnan for discussions on Rietveld refinement and the Robert A. Welch Foundation, Houston, TX for the support of this work.

REFERENCES

1. G. Blasse, "Crystal Chemistry and Some Magnetic Properties of Mixed Metal Oxides with Spinel Structure," thesis, University of Lieden, Apr. 1964.
2. F. Dachille and P. Roy, *Am. J. Sci.* **254,** 722 (1960).
3. A. E. Ringwood and M. Seabrook, *Nature* **193,** 158 (1962).
4. C. Sigala, D. Guyomard, Y. Piffard, and M. Tournoux, *C. R. Acad. Sci. Ser.* 2, **320,** 523 (1995).
5. M. Touboul and A. Popot, *Solid State Chem.* **65,** 287 (1986).

6. K. Mizushima, P. C. Jones, P. J. Wiseman, and J. B. Goodenough, *Mater. Res. Bull.* **15,** 783 (1980).
7. P. G. Bruce, A. Lisokowa-Oleksiak, M. Y. Saidi, and C. A. Vincent, *Solid State Ionics* **57,** 353 (1992).
8. M. M. Thackeray, W. I. F. David, and J. B. Goodenough, *Mater. Res. Bull.* **17,** 785 (1982).
9. M. M. Thackeray, W. I. F. David, P. G. Bruce, and J. B. Goodenough, *Mater. Res. Bull.* **18,** 461 (1983).
10. M. M. Thackeray, S. D. Baker, K. T. Adendroff, and J. B. Goodenough, *Solid State Ionics* **17,** 175 (1985).
11. D. W. Murphy, M. Greenblatt, S. M. Zahurak, R. J. Cava, J. V. Waszaczak, G. W. Hull, and R. S. Hutton, *Rev. Chim. Miner.* **19,** 441 (1982).
12. K. S. Nanjundaswamy, A. K. Padhi, C. Masquelier, and J. B. Goodenough, *in* "Proc. 37th Power Sources Conference, New Jersey, June 1996.
13. G. T. Fey, Wu Li, and J. R. Dahn, *J. Electrochem. Soc.* **141,** 2279 (1994).
14. A. K. Padhi, K. S. Nanjundaswamy, and J. B. Goodenough, *J. Electrochem. Soc.*, in press.
15. K. S. Nanjundaswamy, A. K. Padhi, S. Okada, and J. B. Goodenough, *Solid State Ionics* **92,** 1 (1996).